CHAPTER 6

Magnetic Characteristics of Fe_3O_4 and $Ag@Fe_3O_4$ Nanoparticles

6.1 Introduction

The theoretical and experimental investigation of optical and structural characteristics of the magnetite and silver coated magnetite nanoparticles has been done in the Chapter 3-5. Since the magnetic behavior play a significant role for *in vivo* application of these nanoparticles, in this chapter, we focus on the effect of silver coating on the magnetic properties of Fe_3O_4 nanoparticles and their mutual interactions at the interface. Lots of effort and experiment are being done to regulate the bonding between two different structures in order to produce various morphological nanostructures [25,137,192]. The integration of magnetic nanoparticles with noble metals has given a new dimension in replacement of conventional therapies and diagnostics [193-194].

In this chapter, on the above argument, we report the magnetic investigation of uncoated magnetite nanoparticles with mean diameter of ~6 nm and silver coated Fe_3O_4 nanoparticles with inclusive average particle size ~9 and ~10 nm. The coated samples show a structure where core magnetite nanoparticle is surrounded with thinner than 2 nm

and ~ 2 nm thick silver shells. The magnetic measurements let us observe the variation of blocking temperature, saturation magnetization, magnetically dead layer thickness with respect to shell thickness as well as percentage of superparamagnetic and paramagnetic contribution to the magnetization of the system.

6.2 Temperature Dependent Magnetization Studies

The magnetic properties of synthesized samples have been studied using a Quantum Design Magnetic Property Measurement System (MPMS®). The temperature dependence curve of magnetization under field- cooled and zero- field cooled warming conventions with an externally applied field of 200 Oe is shown in Figure 6.1(a-c). The ZFC measurement was done by cooling down the sample to 2K under zero field and then measuring the magnetization while warming. The FC magnetization data was recorded by cooling the sample to 2K under an applied field of 200 Oe. The figure shows the magnetic behavior of coated and uncoated nanoparticles. The time averages from realizations at higher temperature correspond to the ergodic behavior of the system upto a temperature where curves seem to bifurcate. This point in the curve can be termed as 'ergodicity breaking point' below which the systems behave in entirely two different ways depending upon the cooling field. It indicates that non- ergodic state is achieved at lower temperatures for silver coated magnetite nanoparticles as compared to uncoated ones. The superparamagnetic nanoparticles tend to lose their preferred direction of magnetization in absence of magnetic field at a specific temperature generally termed as blocking temperature (T_b) characterized by maximum of ZFC curve. The blocking temperature (T_b) for 6 nm Fe_3O_4 bare nanoparticle is observed at 106 K. On coating the nanoparticles with silver, the T_b value shifts to 77 K and 69 K on increasing the silver shell thickness.

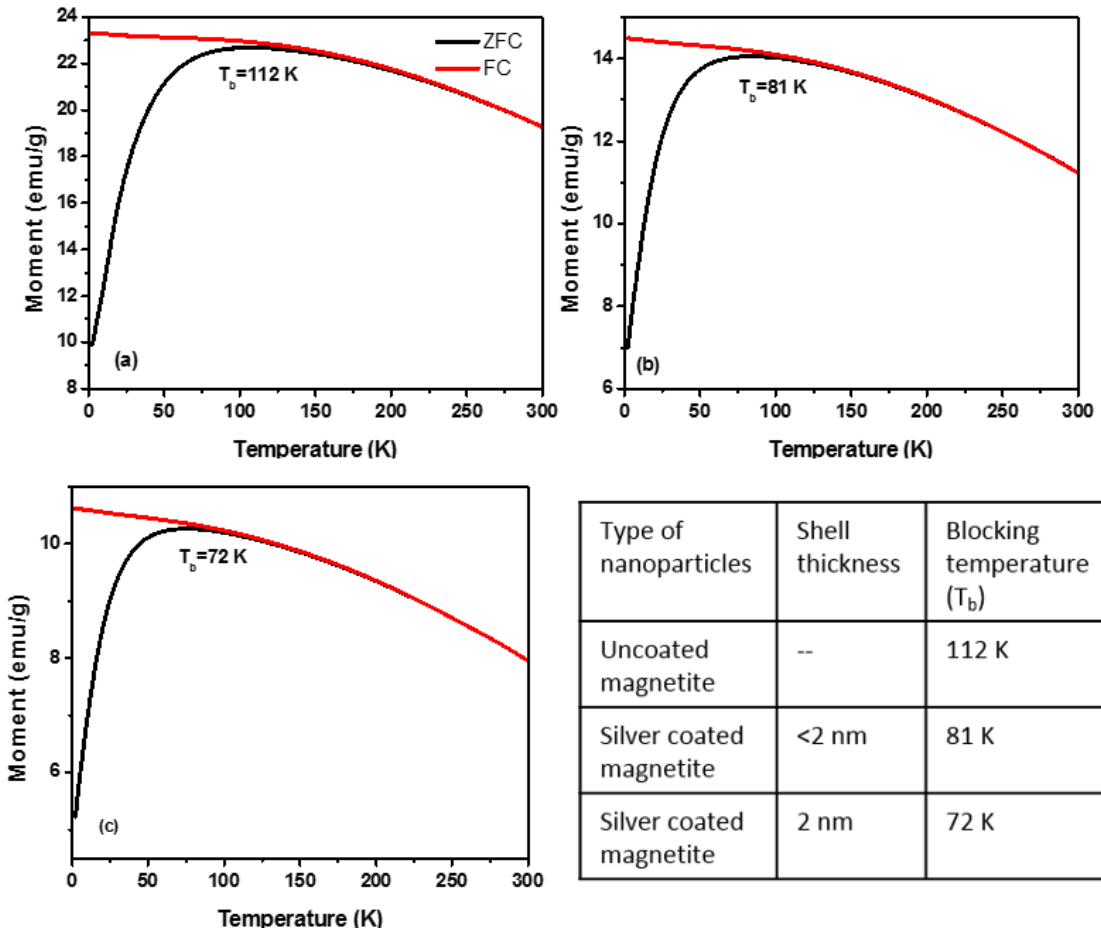

Type of nanoparticles	Shell thickness	Blocking temperature (T_b)
Uncoated magnetite	--	112 K
Silver coated magnetite	<2 nm	81 K
Silver coated magnetite	2 nm	72 K

Figure 6.1 Temperature dependent Zero Field Cooled (ZFC) and Field cooled (FC) magnetization curve for (a) uncoated and (b) thinner than 2 nm shell (c) ~2 nm thick silver shell coated Iron Oxide nanoparticles. The table shows variation of blocking temperature with silver coating.

The table in figure 6.1 shows the dependency of blocking temperature of coated nanoparticles on shell thickness. The value of T_b decreases parabolically with increasing thickness of shell. This decrease in T_b is attributed to a decrease in anisotropic energy with an increase in the thickness of the shell material which is in agreement with the Stoner-Wohlfarth expression used to estimate the average blocking temperature [195]:

$$< T_b > = \frac{K_{eff} * V}{25 * k_B}$$

where, k_B is the Boltzmann constant. The coating with silver nanoshells leads to decrease in coupling of magnetic moments due to interparticle separation of superparamagnetic cores which indicates the reduction of magnetic interactions among the particles upon coating [196]. The effective anisotropy constant values have been calculated using the blocking temperature and effective magnetic volume with the help of equation. The K_{eff} for uncoated magnetite sample is found to be 32.37×10^4 J/m^3 which is in good agreement with reported values for Fe_3O_4 nanoparticles [84]. The anisotropy constant was found to be 23.51×10^4 J/m^3 and 21.07×10^4 J/m^3 for thinner than 2 nm and ~2 nm shell thickness, respectively. The values were found to be decreasing with increase in shell thickness the decrease in values of K_{eff} indicates weak particle-particle interactions for the coated samples which further weakens on increasing the shell thickness. The dipolar interaction energy for a pair of particles is given as [35]: $E_{d-d} = \frac{\mu^2}{r^3}$, where μ and r represent the magnetic moments and center-to-center distance between the particles, respectively. Considering the presence of non-magnetic shell which leads to physical separation between two magnetic particles, a reduction in dipolar interaction energy is observed according to the relation: $\frac{E_{d-d}(\alpha)}{E_{d-d}(0)} \sim \frac{d_{Tem}^3}{(d_{Tem}+\alpha)^3}$ [99]. Here, α is the core-to-core spacing between two coated nanoparticles and d_{Tem} is the average nanoparticle size obtained using TEM. For the case of silver shell thinner than 2 nm coated 6 nm magnetite nanoparticles, $\frac{\alpha}{d_{Tem}} \sim 0.5$, the strength of particle- particle interaction becomes ~29.6 % of $E_{d\text{-}d}(0)$. The occurrence of effective anisotropy constant of nanomaterials can also be related to magnetocrystalline shape and surface anisotropy. Since with increase in shell thickness, the shape remains invariant, the change in K_{eff} is related to the simultaneous effect of surface anisotropy and interparticle interactions. In case of uncoated nanoparticles, they have higher surface spin disorder due to larger number of oxygen ions with incomplete

coordination and broken bonds. The surface effects are highly dominant raising the anisotropy energy constant [196].

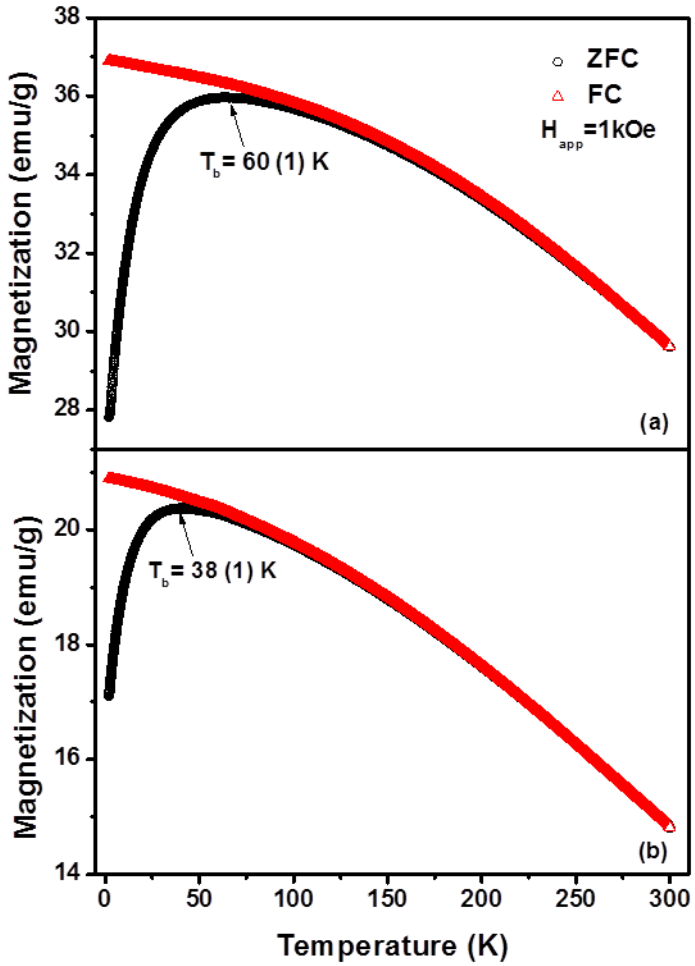

Figure 6.2 Temperature dependent magnetization curve under an applied magnetic field of 1 kOe for (a) uncoated magnetite nanoparticles, and (b) ~2 nm thick silver shell coated magnetite nanoparticles.

The magnetic measurements of ~6 nm uncoated Fe_3O_4 and ~2 nm thick silver shell coated Fe_3O_4 nanoparticles is also carried out as a function of temperature in an applied magnetic field of 1 kOe. The Zero Field Cooled (ZFC) and Field-Cooled (FC) curves of uncoated and coated samples for a cooling field of 1 kOe are shown in Figure 6.2 for a temperature range of 2-300 K. A maximum at 60(1) K and 38(1) K are observed for uncoated and ~2

nm Ag shell coated Fe_3O_4 nanoparticles, suggesting a blocking process at these temperatures, respectively. The absence of kink at lower temperatures discards the existence of Verwey transition in both the samples, probably due to size- effects [84].

The magnetization value of samples at 1 kOe is found to be ~17% smaller than the saturation value which has been identified using magnetization measurement as a function

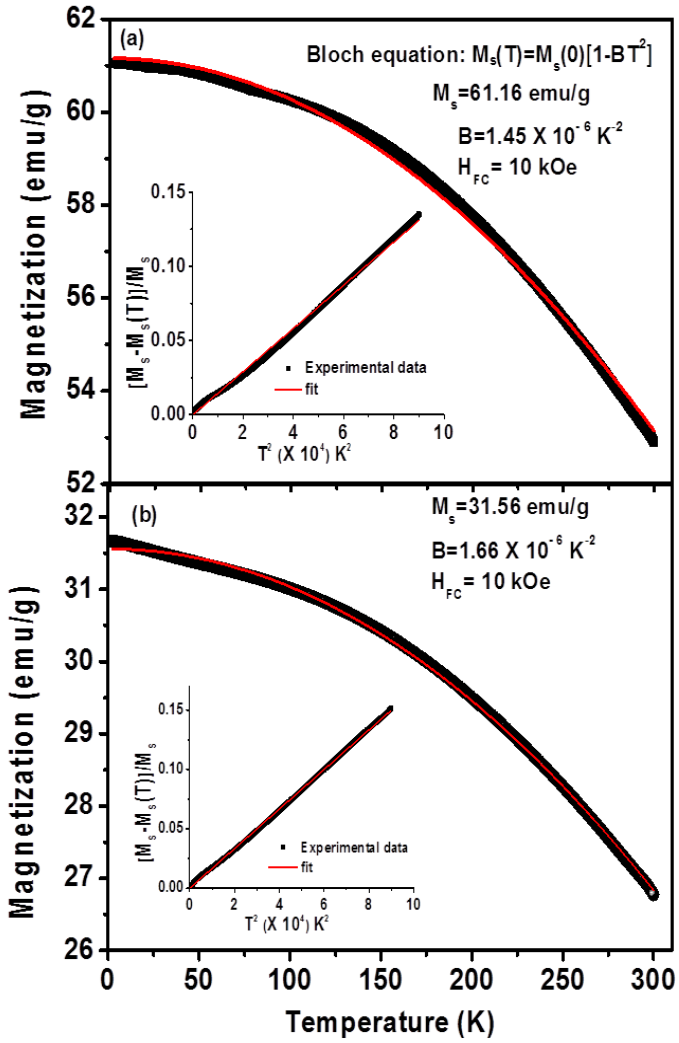

Figure 6.3 Field-cooled magnetization plots under an external magnetic field of magnitude 10 kOe for (a) uncoated magnetite nanoparticles, and (b) ~2 nm thick silver shell coated magnetite nanoparticles. The red line indicates Bloch equation fit for the corresponding data.

of applied field (M-H curve). A steady thermal decrease in magnetization, M of the

samples is observed as shown in Figure 6.3 which is in accordance with a spin wave model consideration of magnetization termed as Bloch law [80]:

$$M_s(T) = M_s[1 - BT^{\alpha}] \quad (1)$$

Here, M_s is the magnetization obtained by extrapolation of M values to zero temperature. B and α represent the Bloch constant and Bloch exponent, respectively. The value of B is a function of exchange integral (J) as $\frac{1}{J^{\alpha}}$. A T^2 dependence of M is observed for both uncoated and coated magnetite samples. A linear relation is inferred between $\frac{[M_S - M_S(T)]}{M_S}$ vs T^2 for both the sets in temperature range 2 K≤ T ≤ 300 K as seen in inset of Figures 6.3 (a) & (b). The Bloch exponent value is in agreement with the values reported using theoretical calculations i.e. $\frac{3}{2} < \alpha < 3$ for smaller ferro- and ferrimagnetic nanoparticles [80]. The value of α increases with reduction in nanoparticle size. The Bloch constant is found to be $1.45 \times 10^{-6}\ K^{-2}$ and $1.66 \times 10^{-6} K^{-2}$ for uncoated and silver coated nanoparticles, respectively, by fitting the experimental data with eq 1. The obtained values are comparable to the data reported earlier [197].

6.3 Field Dependent Magnetization Studies

To investigate the likely effects of shell thickness and exchange coupling between surface and core particles, the hysteresis loops were obtained at 5 K for magnetic field between ±7 Tesla. Figure 6.4 (a), (b) & (c) shows the room temperature hysteresis curve for uncoated Fe_3O_4 and silver shell thinner than 2 nm and ~2 nm silver shell coated Fe_3O_4 nanoparticles, respectively. As seen in figure, the hysteresis loop/ cycles is asymmetric suggesting an occurrence of exchange bias which indicates the presence of exchange coupling between core inner and outer surface. For larger shell thickness, it shows a decrease in saturation magnetization indicating enhanced effects of spin disorder at core surface, resulting in lower net magnetization. The occurrence of magnetic spin disorder

can be related to breaking of symmetry and broken bonds at the interface leading to magnetic frustrations. When the system is subjected to lower temperature, at the time of spin reversal of ordered region, the oriented spins behave as pinning agents resulting shift in hysteresis loop. This type of exchange anisotropy field due to disorder in magnetic spin layer at the surface has been reported in core-shell systems [198]. Highly magnetic disordered layer in inner and outer surface of magnetic core accounts for strong exchange bias observed in coated iron oxide nanoparticles [199].

The minimal values of coercivity and remanence at 300 K indicate the superparamagnetic behavior of the particles. The saturation magnetization (M_s) for uncoated magnetite nanoparticles is observed to be 63 emu/g which nearly match the data reported earlier [49]. The decrease in M_s value is observed upon coating of the magnetite NPs with silver which is quite obvious. The magnetic moment values are corrected by considering the weighted fraction of Fe_3O_4 in the core- shell nanostructures using quantity of silver required during synthesis to coat the magnetite nanoparticles with given shell thickness. It gradually decreases from 55 emu/g to 53 emu/g with increasing shell thickness corresponding to thinner than 2 nm and ~2 nm, respectively. The magnetite nanoparticles of size 12±3 nm with silver shell coating of thickness 2±1 nm has been reported to show the reduction of magnetization value by 20 times for coated magnetic particles as compared to uncoated ones [200]. In this case, the M_s value of uncoated magnetite nanoparticles is reduced by 29% and 26% of bulk magnetite (M_s (bulk): at 5 K = 88.5 emu/g; at 300 K= 75.6 K [84]) due to decreased particle size and increased surface to volume ratios.

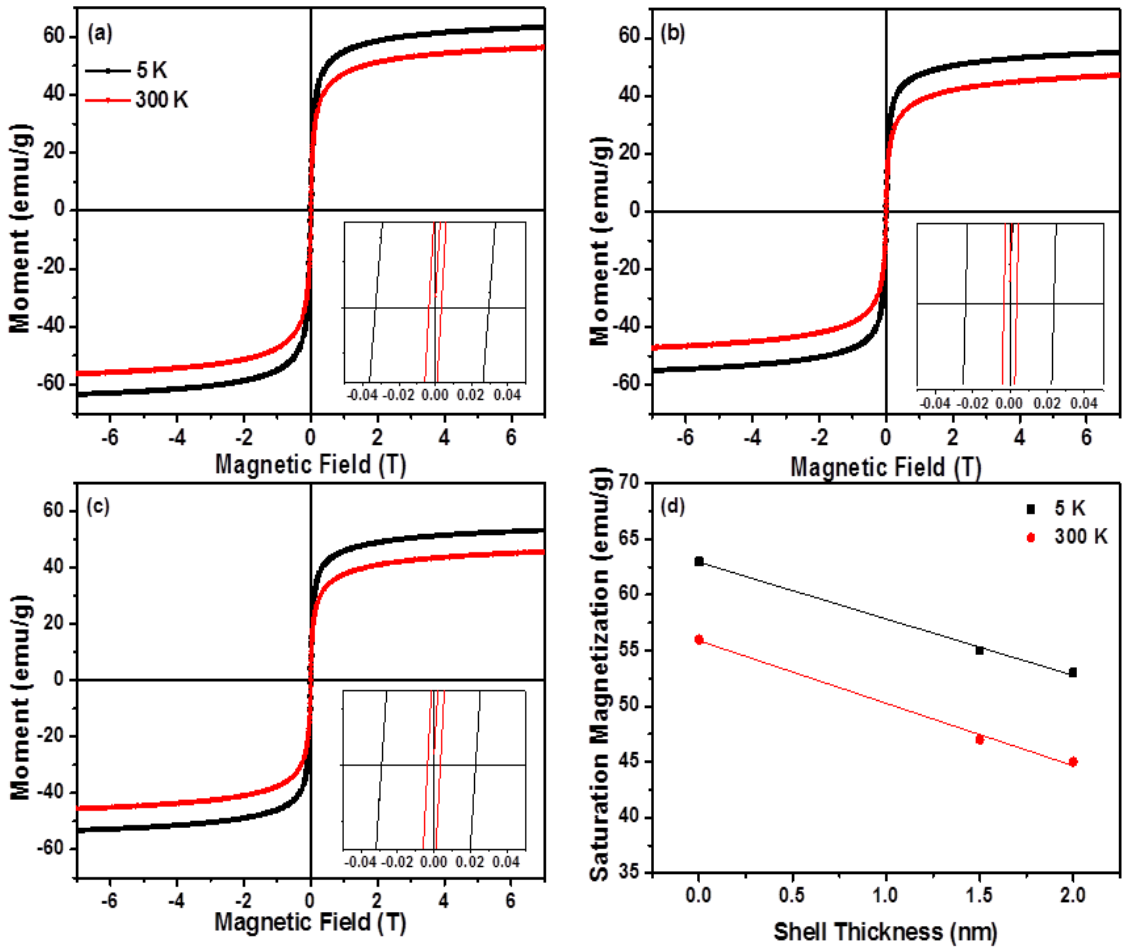

Figure 6.4 Field dependent magnetization curve at 5 K and 300 K for (a) uncoated and (b) thinner than 2 nm, (c) ~2 nm silver coated magnetite nanoparticles, (d) Variation of saturation magnetization with respect to shell thickness.

The magnetization measurements with varying magnetic field at different temperatures are performed to probe the temperature at which the uncoated and ~2 nm thick silver shell coated magnetite nanoparticles attain perfect superparamagnetic behavior state. The MH curve for Fe_3O_4 and $Ag@Fe_3O_4$ in temperature ranges 5 to 300 K shows that both of these nanoparticles exhibit perfect superparamagnetism state at 100 K. The magnetization saturates at ~40 kOe for both the systems. As shown in Figure 6.5 (a) & (b), the hysteresis loops are symmetrical within experimental error that discards any possibility of exchange

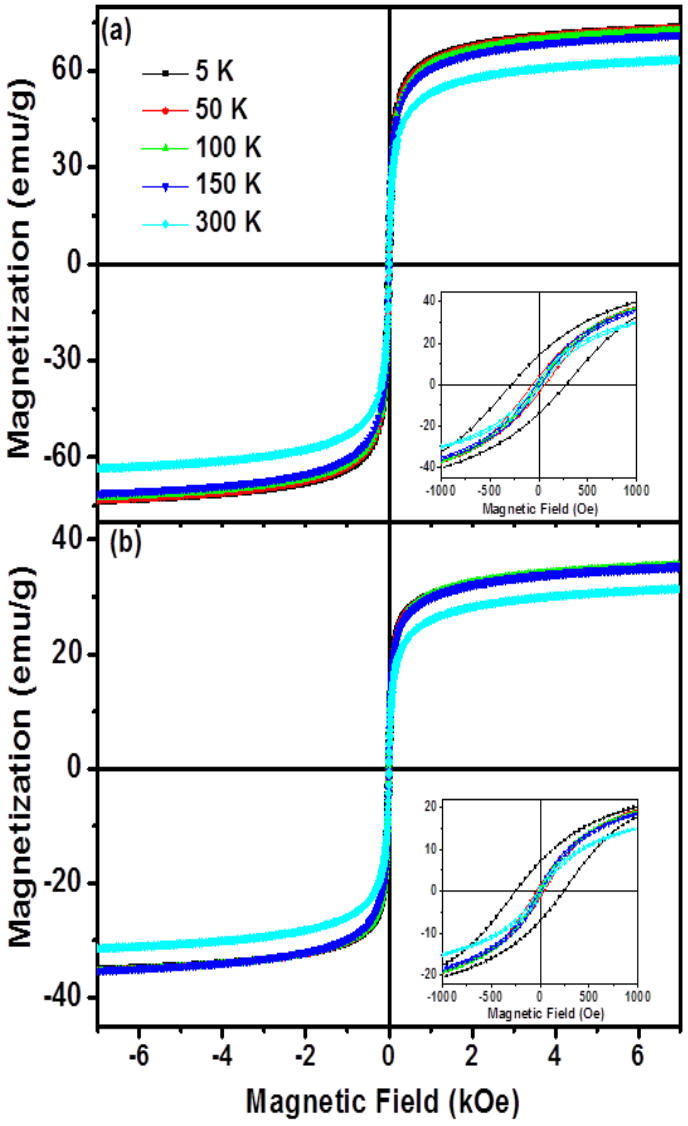

Figure 6.5 Field dependent magnetization curves at five different temperatures in field range of ± 7 kOe for (a) uncoated Fe_3O_4 nanoparticles (b) ~2 nm thick silver shell coated Fe_3O_4 nanoparticles. The inset shows magnified curve in range ± 1 kOe with perfect superparamagnetic behavior at 100 K for both the samples.

coupling for uncoated and coated magnetite nanoparticles. The decrease in saturation magnetization indicates the increasing effects of spin disorder in coated nanoparticles which is responsible for smaller values of magnetization. An oxygen ion mediates the exchange interaction (superexchange) between the two adjacent ferrous/ ferric ions. If an

oxygen ion is absent from the surface/ interface, the interaction energy is reduced due to broken exchange bonds. There is a possibility of decrease in average coordination number for the iron ions at the surface/ interface which may further lead to wider distribution of

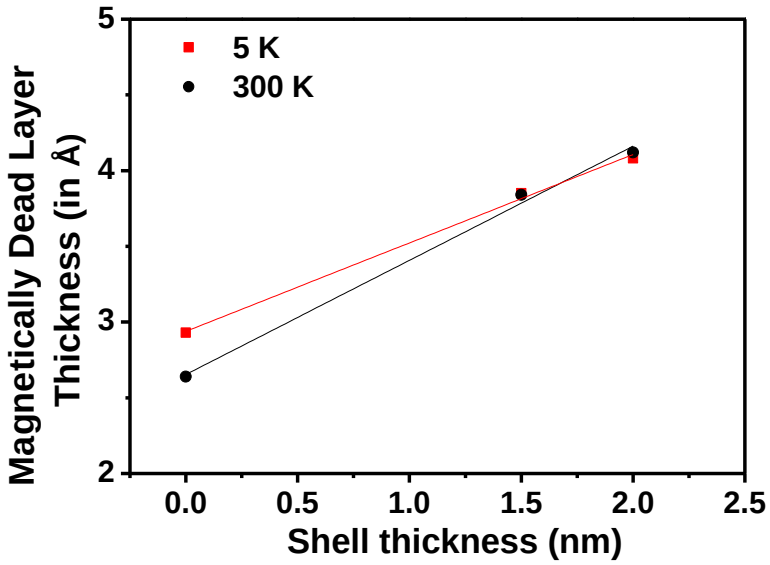

Figure 6.6 Variation of Magnetically Dead layer thickness as a function of silver shell thickness.

exchange energies for spins at the surface for uncoated nanoparticles and interface spins for coated nanoparticles. These factors lead to development of surface spin-disordered systems.

The decrease in the M_s value of coated NPs due to the presence of a diamagnetic shell on the surface of magnetic core reduces the magnetic moment due to the interaction of silver shell with magnetic core at interface and shielding effects of shell material. A magnetically dead layer on surface appears due to decrease in coordination as well as absence of oxygen causing reduction of M_s values when compared to that of bulk sample. The thickness of magnetically dead layer (t) is calculated using the formula [97]:

$$M_s = M_s(bulk)\left(1 - \frac{6t}{D_{Tem}}\right)$$

Using the values of average particle size obtained using TEM (D_{Tem}), saturation value of bulk magnetite (M_s (bulk): at 5 K = 88.5 emu/g; at 300 K= 75.6 K [38]) and saturation value obtained for uncoated and coated sample (M_s), we obtained '*t* ' values at two temperatures 5 K and 300 K for each sample.

The thickness of magnetically dead layer for ~6 nm uncoated magnetite nanoparticle is found to be 2.93 Å at 5 K and 2.64 Å at 300 K. Upon coating with thinner than 2 nm silver shell, the thickness of layer enhances to 3.85 Å (5 K) and 3.84 Å (300 K). It further rises to 4.08 Å (5 K) and 4.12 Å (300 K) for ~2 nm thick silver shell coated magnetite nanoparticles as shown in Figure 6.6. This quantitative increase in the thickness of magnetically dead layer accounts for the reduction in saturation magnetization for uncoated and coated nanoparticles as compared to the bulk magnetite nanoparticles.

6.4 Contribution of Superparamagnetic and Paramagnetic Behavior in Uncoated and Ag Coated Fe_3O_4 Nanoparticles

The Langevin function to analyze the magnetization of SPM nanoparticles in an externally applied magnetic field H is given as [51]:

$$M\,(H) = M_s^{spm} L\left(\frac{\mu H}{k_B T}\right)$$

To realize the significance of disordered magnetic spin layer, we have splitted the paramagnetic and superparamagnetic contributions to value of magnetization by fitting the MH data of uncoated and coated samples at room temperature by addition of a linear term. The modified Langevin equation is stated as following expression [98]:

$$M\,(H) = M_s^{spm} L\left(\frac{\mu H}{k_B T}\right) + PH$$

Where M_s^{Spm} denotes M_s value of superparamagnetic part, μ is the average magnetic moment and P is the paramagnetic contribution to the susceptibility varying with field. Figures 6.7 (a) & (b) shows the experimental and fitted curves. It can be observed that for

uncoated particles (particle size = 6 nm), the superparamagnetic contribution to the susceptibility is 91% of the total magnetic moment obtained experimentally, while remaining 9% is due to the paramagnetic behavior of the uncoated magnetite nanoparticles. On coating of these magnetite nanoparticles, the contribution from paramagnetic susceptibility is raised to 17% whereas the superparamagnetic susceptibility contributes 83% of the total observed magnetic moment for coated ones. The increased value of paramagnetic susceptibility shows contribution from uncompensated spins at core- shell interface and particle surfaces leading to pinning of spins along local axis resulting due to surface anisotropy. The greater contribution of paramagnetic susceptibility to magnetization points towards strong disordered effect of spins for coated magnetite nanoparticles.

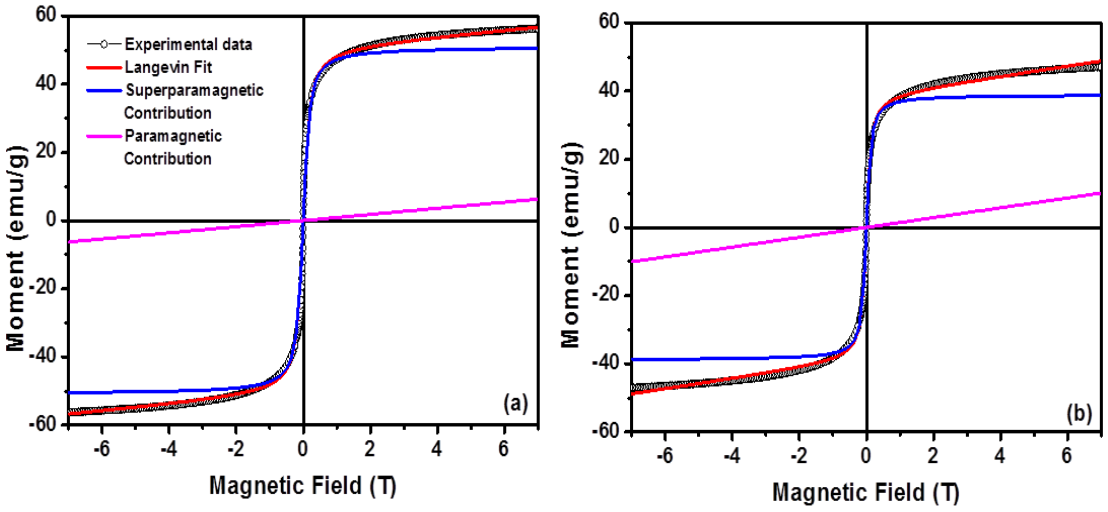

Figure 6.7 M-H curves at room temperature for coated and uncoated magnetite fitted to equation 4 (red); the blue and green curves show calculated SPM and PM contributions obtained from the experimental values obtained as fitting parameters: (a) ~6 nm uncoated magnetite nanoparticles; (b) thinner than 2 nm silver shell coated nanoparticles.

The structural analysis from XRD data of the uncoated and silver-coated magnetite nanoparticles, in chapter 4 shows expansion of lattice parameters *'a'* for Fe_3O_4 nanocore structure in case of coated nanoparticles which is consequence of diffusion of silver ions inside the magnetite unit cell. The increasing value of *a* is due to larger ionic radii of silver. The depth of core layer until which this type of diffusion occurs is finite forming a disordered spin layer in between magnetic core and non-magnetic shell. This prediction of trilayer structure has also been analyzed using magnetic data. There are three such possible structures for coated nanoparticles: bilayer structures with (i) magnetic Fe_3O_4 core and non-magnetic silver shell (ii) completely silver diffused core with non-magnetic silver shell (iii) trilayer structure with magnetic core surrounded by a disordered magnetic shell and silver as outermost layer. The different values of blocking temperature and saturation magnetization is obtained for ~6 nm uncoated magnetite and ~ thinner than 2 nm & ~2 nm thick silver coated nanoparticles. The variation in these values for uncoated and coated nanoparticles discards our first assumption of bilayer structure. The coated and uncoated nanoparticles should show nearly equal value of T_b as well as M_s since the silver shell surrounding the magnetic core is completely non-magnetic having nil contribution to these values. Now, considering the values of M_s and T_b for magnetite nanoparticles coated with two different thick shells, we can say that if the core is completely diffused, these values should be constant irrespective of the shell thickness as the size of diffused core is same for both samples and outermost layer is diamagnetic in nature. The values obtained for two different shells are not in agreement with the above statement. Thus, the assumption of this bilayer structure is also eliminated. Since the silver diffuses inside the core up to some depth a disordered spin layer is formed in between the magnetic core and non-magnetic shell. The thickness of this layer varies with the thickness of coated shell material that leads to change in values of T_b and M_s for coated

materials and absence of this layer in uncoated magnetite is responsible for higher magnetization values as compared to coated ones. Thus, from these structural and magnetic data analysis, we can state that structure is not exactly core-shell but a structure with magnetic core surrounded by a disordered magnetic shell and silver as outermost layer.

6.5 Conclusions

Silver coated magnetite nanoparticles with various shell thickness using microemulsion technique has been synthesized. The mean particle size of magnetite core was found to be 6 nm and coated shells of thickness thinner than 2 nm and ~2 nm as measured by transmission electron micrographs. Another polydispersed Fe_3O_4 @Ag nanoparticle sample was prepared with average shell thickness of ~9 nm to show the effect of polydispersion from PL spectra. The ZFC- FC curves for varying shell thickness reveal the decrease in blocking temperature ultimately leading to reduction of effective anisotropy constant arising due to simultaneous effect of surface anisotropy and inter-particle interactions. The M-H curves at 5 K and 300 K confirmed the superparamagnetic nature of the synthesized samples. The value of M_s was found to be decreasing almost linearly with shell thickness. The interaction of silver shell with magnetic core and shielding effect of non- magnetic material is the reason behind this magnetic behavior. The increase in thickness of magnetically dead layer at interface is also a prominent cause. From structural and magnetic analysis, we report that the structure is not exactly bilayer core- shell but a structure with disordered magnetic shell in between magnetic core and outermost silver layer. The reason behind this argument is diffusivity of silver inside the magnetic core. The difference in the values of T_b and M_s for uncoated and silver coated magnetite nanoparticles confirms our assumption of the structure. In all, we conclude that the structural and magnetic sensitivity of these coated nanoparticles alter up to a

considerable extent when compared to the uncoated ones of same magnetic core size. The coating with non-magnetic material affects the magnetization of coated materials due to surface moments quenching. The saturation magnetization values are much higher for thin shell coatings. These excellent magnetic properties make them suitable material for target specific drug deliveries or carriers. In addition, since the value of relaxivity is directly proportional to the saturation magnetization, the magnetite nanoparticles with thinner shells are an exquisite option as T_2 contrast agents. This requires further in vitro relaxivity studies of the silver coated samples to strengthen the claim of their applicability for contrast enhancement agents.

Along with these magnetic properties, the magnetic spin relaxation plays a significant contribution in these applications. For this purpose, the dynamics of magnetic spins need to be explained which involves several magnetic relaxation measurements. The next chapter deals with the spin dynamics of magnetite and magnetite-silver core-shell nanoparticles.